

Entangled photon apparatus for the undergraduate laboratory

Dietrich Dehlinger, M. W. Mitchell

*Physics Department, Reed College 3203 SE Woodstock Blvd.
Portland, OR 97202**

We present detailed instructions for constructing and operating an apparatus to produce and detect polarization-entangled photons. The source operates by type-I spontaneous parametric downconversion in a two-crystal geometry. Photons are detected in coincidence by single-photon counting modules and show strong angular and polarization correlations. We observe more than 100 entangled photon pairs per second. A test of a Bell inequality can be performed in an afternoon.

I. INTRODUCTION

Entanglement of particles is ubiquitous in quantum mechanical systems and is arguably the aspect of quantum theory most at odds with classical intuitions. Einstein, Podolsky and Rosen first drew attention to the possibility of non-local effects involving entangled particles.¹ In the mid-Sixties it was realized that the nonlocality of nature was a testable hypothesis and subsequent experiments confirmed the quantum predictions. More recently, much effort has gone into exploiting the odd nature of entangled particles.² Applications include secure cryptography, transmission of two bits of information with a single photon and “teleportation” of a quantum state (by erasing the state of a system and then re-creating the state in a distant system).^{4,5,6,7,8} Perhaps the most exciting possible application is in computing. A “quantum computer” which used entangled particles as data registers would be capable of performing calculations faster than any classical computer.^{11,12,13,14}

Here we describe how to produce and detect entangled photons using equipment and techniques suitable for an undergraduate laboratory. This is possible due to recent advances in diode laser technology and new techniques for generation of photon pairs.^{15,16} The total cost for the apparatus is approximately 15,000 USD.

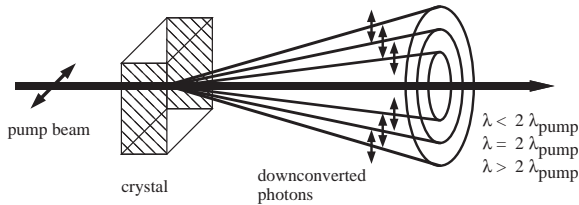


FIG. 1: Type I spontaneous parametric downconversion. Photons from a pump beam split into pairs of photons.

II. OVERVIEW

In the process of spontaneous parametric downconversion (SPD) a single pump photon spontaneously splits into “signal” and “idler” photons inside a nonlinear crystal.^{17,18} Because the two downconverted photons come from a single parent photon they have definite combined properties: their total energy

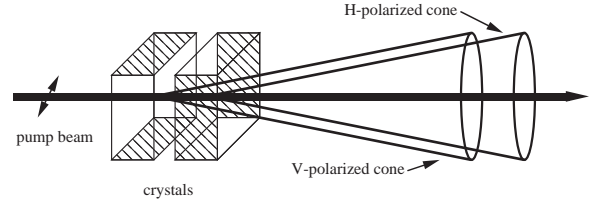


FIG. 2: Two-crystal downconversion source.

and momentum (inside the crystal) must agree with the parent energy and momentum. They are also produced at very nearly the same time. The individual photons’ properties are free to vary, however, and SPD produces a spectrum of both signal and idler wavelengths centered around twice the parent photon wavelength. To satisfy phase matching requirements, which reflect the dispersion and birefringence of the crystal, these different wavelengths emerge in different directions and create a conical rainbow of emission as illustrated in Figure 1.

By appropriate angular placement of the detectors, we select “degenerate” daughter photons, those which have the same wavelength $\lambda_S = \lambda_I = 2\lambda_{\text{pump}}$. Our crystals are cut for Type I downconversion, in which the signal and idler photons have the same polarization, which is opposite to that of the pump photon.¹⁹ A given crystal can only support Type I downconversion of one pump polarization, the other polarization simply passes through the transparent crystal. Our source uses two identical crystals, with one rotated 90° from the other about the beam propagation direction, as shown in Figure 2. In this arrangement each crystal can support downconversion of one pump polarization. A 45° polarized pump photon can downconvert in either crystal, producing a polarization-entangled pair of photons.¹⁶

Figure 3 shows a schematic of the experimental setup. A 5 mW, 405 nm, InGaN laser diode (Nichia Model NLHV500C) is the source of pump photons. The diode is driven at its specified operating current with a precision constant current source capable of supplying the 5V operating voltage of the InGaN laser. The beam is focused with an aspheric lens mounted in a collimating tube, which is held in a vee-mount glued to a mirror mount. The beam focus is adjusted to produce a beam diameter of about 1 mm at 1 m from the laser.

The laser beam passes a BG12 colored glass filter, a beam aperture consisting of a sheet of aluminum with small hole

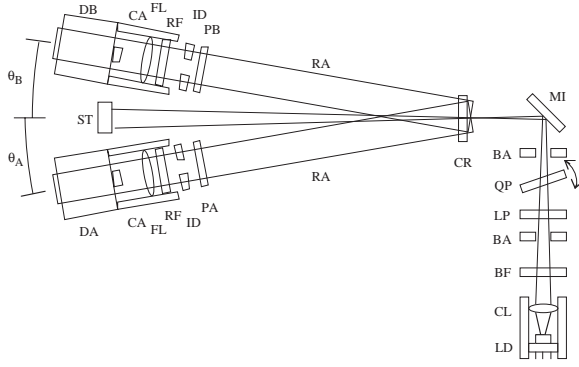


FIG. 3: Schematic diagram of experimental setup, not to scale. Symbols: LD Laser Diode, CL Collimating Lens, BF Blue Filter, BA Beam Aperture, LP Laser Polarizer, QP Quartz Plate, MI Mirror, CR Downconversion Crystals, RA Rail, PA Polarizer A, PB Polarizer B, ID Iris Diaphragm, RF Red Filter, FL Focusing Lens, CA Cage Assembly, DA Detector A, DB Detector B, ST Beam Stop.

drilled in it, a glass linear polarizer on a rotating mount, a 0.5 mm thick quartz plate mounted to rotate about the vertical (the crystal's fast axis) and a second beam aperture before reaching the nonlinear crystals. The apertures and filter act to remove unwanted light and the polarizer and quartz plate set the laser polarization.

The nonlinear crystals are two beta barium borate (BBO) crystals, 5 mm \times 5 mm \times 0.1 mm thick, cut with their crystal axes at 29° from normal to the large face. The crystals are mounted face-to-face with one crystal rotated by 90° about the normal to the large face. The crystal holder is held in a mirror mount and aligned to retroreflect the laser beam. A beam stop blocks the laser beam after it passes alongside the detectors.

The downconverted photons produced in the BBO crystals travel about 1 meter before passing an adjustable 1 inch diameter iris diaphragm, a plastic film near-infrared polarizer on a rotatable mount, a 1 inch diameter RG780 colored glass filter, and are focused by a 75mm focal length lens onto the detector surface. The RG780 is a long-pass filter with a 50% transmission at 780 nm. For a coincidence detection event to occur, both signal and idler photons, which are roughly equally spaced in wavelength about 810 nm, must pass RG780 filters. Thus a wavelength band (in the signal photon) of about 780–840 nm can lead to coincidence detection.

The detectors (Perkin-Elmer Optoelectronics model SPCM-AQR-13) are silicon avalanche photodiodes run in Geiger mode, called single-photon counting modules (SPCMs).^{20,21}

To aid in focusing, each detector was mounted on standard optical mounting posts and a 30 mm “cage” assembly was attached to hold the lens and RG780 filter. These are described in section III. The lens is held in an X-Y translator for fine adjustment of the lens position.

Along each detection path, the detector, lens, filter, polarizer and iris are mounted on an aluminum rail which pivots about an optical post directly below the crystal. This arrangement allows adjustment of the angular position of the detec-

tors without losing focus. Although we performed our experiments on an optical table, we note that this is probably unnecessary. Interferometric stability is not required and the rails maintain the necessary alignment. We expect the experiment could be performed on an optical breadboard or other flat surface.

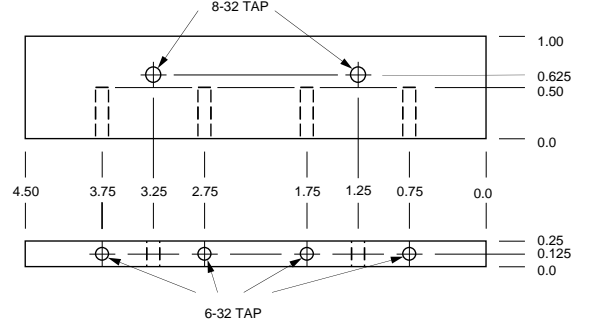


FIG. 4: SPCM base adapter plate. Units: inches, all tolerances are ± 0.01 inch unless otherwise specified.

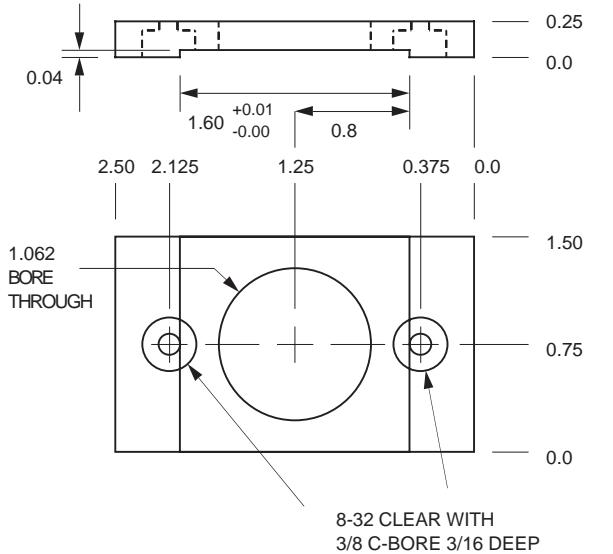


FIG. 5: SPCM front adapter plate. Units: inches, all tolerances are ± 0.01 inch unless otherwise specified.

III. MECHANICS

The first version of the detection setup used independent table-mounted components to hold the filters and position the focusing lenses. This early setup was quick to assemble from common components such as translation stages and lens holders, but was difficult to align and required near-complete darkness. For greater ease of use we developed the mechanical system described below.

The SPCMs, as furnished by the manufacturer, do not directly interface to standard optical hardware. We built two

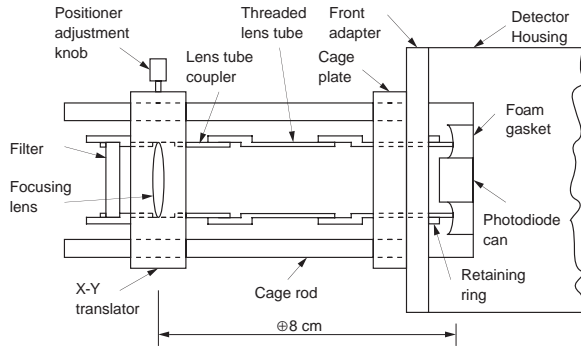


FIG. 6: Schematic diagram of detector-mounted cage assembly, side view.

simple adapter plates, shown in Figures 4 and 5. The base adapter allows the detector to be mounted on standard optical posts, while the front adapter allows a cage assembly to be attached to the detector, as shown in Figure 6. The cage assembly consists of four rods, each 4 inches long, held at the detector end by a 30 mm cage plate and at the other end by a 30 mm X-Y translator which holds the focusing lens and filter. The cage plate attaches to the front adapter by a threaded tube and a retaining ring. This same tube presses against a gasket of black closed-cell foam to make a light-tight seal. Other threaded tubes link the X-Y translator to the cage plate. This arrangement has two principal advantages. First, the path from filter to detector is entirely enclosed, greatly reducing sensitivity to stray light and protecting the detector from mechanical damage. Second, precise positioning of the focusing lens is easily accomplished by sliding the X-Y translator along the rails and adjusting the X-Y translation knobs. Because the lens sits about 1m away from the crystals, the image of the crystals on the detector moves by about $75 \mu\text{m}$ for every 1 mm displacement of the lens. This is handy as the detector area is only $180 \mu\text{m}$ in diameter.

Each detector and cage assembly, as well as the associated iris and polarizer, sit upon a detector rail as shown in Figure 3. We constructed our rails from half-inch thick aluminum bars, as shown in Figure 7. Four post holders are mounted directly to the rail to hold the detector, iris, and linear polarizer. A half-inch diameter hole at the opposite end from the detector fits over a standard (0.499 inch diameter) optical post which serves as a pivot for the rail. The second rail pivots about the same post, sitting upon the first rail. A half-inch high spacer beneath the second rail on the detector end allows the rail to sit flat on the table.

IV. ELECTRONICS

Detection of a photon by an SPCM produces a short (about 25 ns) TTL pulse. To identify photons from SPD within the background of fluorescence photons, we record coincident detections. Our first coincidence detector used a NIM standard time-to-amplitude converter and a multi-channel analyzer (MCA). This setup required converting the TTL pulses

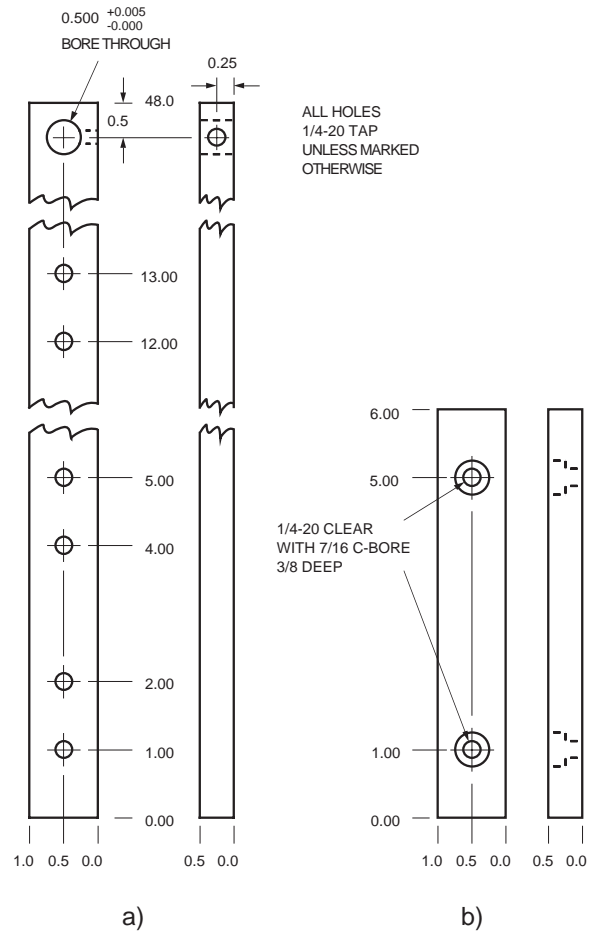


FIG. 7: Detector rail. a) rail b) under-rail spacer. All parts are aluminum. Units: inches, all tolerances are ± 0.01 inch unless otherwise specified.

to NIM pulses and also required a computer to record data from the MCA. A simpler and far less expensive alternative is to build a coincidence circuit from fast logic chips. A schematic for such a circuit is shown in Figure 8.

The circuit is built from two 74ACT74 dual D-type positive edge-triggered flip-flops, or four D-type flip-flops in all. Starting at the lower left of the diagram and working clockwise, the first flip-flop delays the B pulse by the time required to clock and reset, 6.5 ns to 19.5 ns by the manufacturer's specifications. The next flip-flop produces a stretched pulse at A OUT. The next performs the coincidence detection: If A IN is already high when the delayed B pulse arrives, a stretched pulse is produced at COINC OUT. The coincidence window is the duration of the A IN pulse. The final flip-flop stretches the B pulse. The inputs are 50Ω terminated. The output pulses are all TTL compatible and about 250 ns long. Longer pulses can be produced by increasing the values of the capacitors. The output pulses are fed to the counter-timer inputs of a PC-based data acquisition board.

The coincidence circuit is simple to build, but as with any fast electronics, proper construction technique is necessary for good performance. It is helpful to have a fast oscilloscope

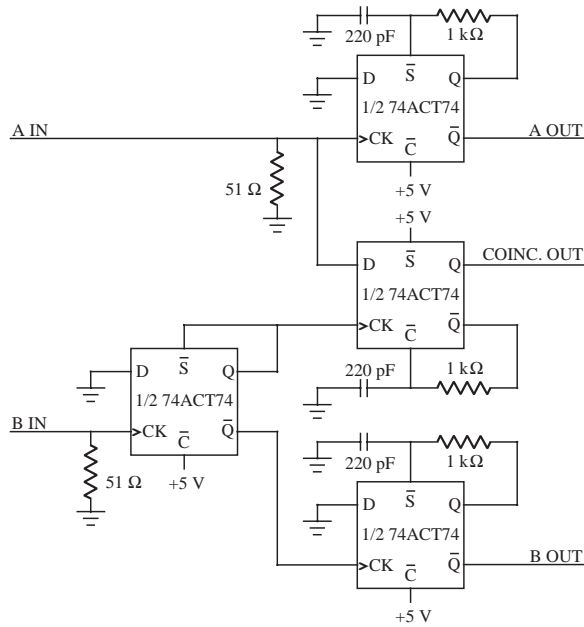


FIG. 8: Schematic diagram of coincidence detection circuit. See text for details.

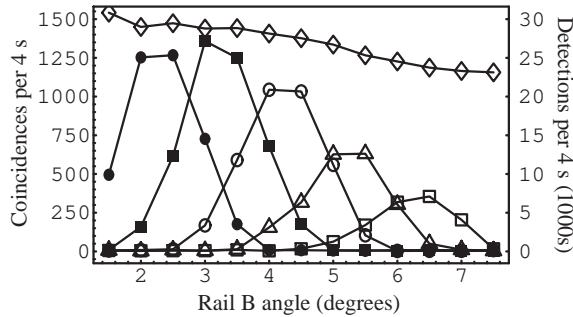


FIG. 9: Coincidence and singles detection rates as a function of detector positions. Solid circles, solid squares, hollow circles, hollow triangles and hollow squares show coincidence rates for $\theta_A = 2^\circ$, 3° , 4° , 5° , and 6° , respectively, on left scale. Diamonds show channel B detection rate on right scale.

when debugging this circuit.

V. ALIGNMENT

The apparatus is not difficult to align if done in the correct order. All optical elements should be set to the same height above the table. With the crystals, polarizers and RG780 filters removed from the setup, the remaining rail-mounted components (detectors, lenses, and irises) can be aligned as follows. The detector is viewed from the position the crystals will occupy, through the open iris and lens. The detector's active area is a circular black spot at the center of a gold square. By aligning and focusing the lens, the detector's active area can be made to fill the field of view. The iris should be centered on this image.

Once this rough alignment is performed, the crystals, polarizers and RG780 filters can be put in place. The laser is aligned to pass through the crystals' center. The rails should be positioned on opposite sides of the laser beam, each about three degrees away from the beam. With the room darkened, fine adjustments in lens position can be made to maximize the singles count rate at each detector. Finally, the angles of the rails should be adjusted to maximize the coincidence detection rate. Following this procedure we find coincidence rates greater than 300 cps, as shown in Figure 9.

To show that the photons are polarization-entangled, we measured coincidence rates as a function of the two polarizer orientations. The polarization correlations were strong enough to demonstrate a violation of a Bell inequality. We used the Clauser, Horne, Shimony and Holt version of the Bell inequality $|S| \leq 2$, where S is a measure of the polarization correlation involving sixteen coincidence measurements. As described in the accompanying paper, we found $S = 2.307 \pm 0.035$, a clear violation.²² The total acquisition time in this experiment was 240 seconds and a fit to the coincidence data indicates more than 100 polarization-entangled photons per second. These data were taken with the irises fully opened. Closing down the irises will reduce the count rate, but may improve the purity of the detected entangled state.

VI. MISCELLANEOUS

A darkened room is necessary for the experiment but complete darkness is neither necessary nor desirable. In our setup, black velvet curtains surrounding the work area block out sunlight and room lights. We find a dimmed but visible computer monitor adjacent to the optical table gives negligible background coincidence counts. We use green LEDs behind BG-18 colored glass filters to illuminate the table; the green light is blocked by the RG780 filters.

VII. ACKNOWLEDGEMENTS

We thank Paul Kwiat for inspiration and helpful discussions. This work was supported by Reed College and grant number DUE-0088605 from the National Science Foundation.

APPENDIX A: SUPPLIERS AND EQUIPMENT NOTES

Below we list components of the apparatus which are unique or difficult to find, as well as suppliers for these components. These are also the most costly parts of the apparatus. Remaining components not described below include standard optical hardware such as mirror mounts, electronics to build the coincidence detector, and a means to record the detection rates.

Edmund Industrial Optics
101 East Gloucester Pike

Barrington, NJ 08007-1380
(800) 363-1992
<http://www.edmundoptics.com>

25.4 mm diameter unmounted linear glass polarizing filters. 1"×1" Polaroid near-IR linear polarizing film ×2. 1" diameter RG-780 colored glass longpass filter ×2. 1" diameter BG-12 blue-violet colored glass bandpass filter. 1" diameter BG-18 blue-green colored glass bandpass filter. Total cost: \$255.

ILX Lightwave
P.O. Box 6310
Bozeman, MT
(800) 459-9459
<http://www.ilxlightwave.com>

LDX-3412 Precision Current Source. Cost: \$846.

This model was chosen both for its precision and its compliance voltage. Most diode laser drivers can't supply the 5V operating voltage of the gallium nitride laser.

MTI Corporation
5327 Jacuzzi St. Bldg. 3H
Richmond, CA 94804
(510) 525-3070
<http://www.mticrystal.com>

SO*10 x-cut 5mm×5mm×0.5mm quartz substrate, optically polished on both sides. Cost: \$12.

We glued this piece of quartz to a metal support to mount in an optic holder.

Nichia Corporation
Tokyo technical center
13F Tamachi Center Building, 34-7, Shiba 5-Chome
Minato-Ku, Tokyo 108-0014
Japan
<http://www.nichia.co.jp>

NLHV500C: 5mW nominal wavelength 405 nm InGaN laser diode, 1000 hour version. Cost: \$1000.

We tested two diodes, one with a wavelength of 400 nm, the other 406 nm, with very similar results. As InGaN laser diodes are a very young technology, it is reasonable to expect

improvements in cost and lifetime in the near future.

Perkin-Elmer Optoelectronics
22001 Dumberry Road
Vaudreuil Quebec J7V 8P7
CANADA
(450)-424-3300
<http://opto.perkinelmer.com>

SPCM-AQR-13 Silicon APD Based Single Photon Counting Modules ×2. Total cost: \$7200.

The -13 suffix describes the dark count rate. This has very little effect upon the coincidence count rate in the experiment, and any suffix model can be used. Note that the lead time for these detectors can be several months. Detectors require a +5 Volt power supply, not included.

Thorlabs, Inc.
435 Route 206
P.O. Box 366
Newton, NJ 07860
(973) 579-7227
<http://www.thorlabs.com>

C230TM-A: 0.55 NA aspheric lens, AR coated 350-600nm. Collimating tube for 5.6mm laser diode and C230TM-A. S7060: Laser diode socket for 5.6mm laser. VC1 V-Clamp SPW301: 3/8" Spanner wrench. SPW602: SM1 Series Spanner wrench. CP02: 30mm Threaded cage plate ×2. HPT1: 30mm cage X-Y translator ×2. ER4: Extension rod, 4" long ×8. SM1V10: 1" adjustable focus tube for 1" optics ×4. SM1V05: 1/2" adjustable focus tube for 1" optics ×2. SM1T2: SM1 coupler, external threads ×2. RSP1: Rotation stage for 1" optics ×3. Total cost: \$1040.

U-oplaz Technologies
21828 Lassen St, #D
Chatsworth, CA 91311
(818) 678-1999
<http://www.u-oplaz.com>

Two identical β -barium borate (BBO) crystals, 5mm×5mm×0.1mm with a crystal cut of 29°, protective "P-coating." Crystals custom-mounted face-to-face with one crystal rotated by 90° in a standard mount. Cost: \$1400.

* Electronic address: morgan.mitchell@reed.edu

¹ A. Einstein, B. Podolsky, and N. Rosen, "Can quantum-mechanical description of physical reality be considered complete?," *Phys. Rev.* **47**, 777-780 (1935).

² J. S. Bell, *Physics* (Long Island City, NY) **1**, 195-200 (1964). This article is reprinted in³.

³ J. A. Wheeler and W. H. Zurek, *Quantum Theory and Measurement* (Princeton University Press, Princeton, NJ, 1983).

⁴ A. K. Ekert, "Quantum cryptography based on Bell's theorem," *Phys. Rev. Lett.* **67**(6), 661-663 (1991).

⁵ T. Jennewein, C. Simon, G. Weihs, H. Weinfurter and A. Zeilinger, "Quantum cryptography with entangled photons," *Phys. Rev. Lett.* **84**(20), 4729-4732 (2000).

⁶ D. S. Naik, C. G. Peterson, A. G. White, A. J. Berglund and P. G. Kwiat, "Entangled state quantum cryptography: Eavesdropping on the Ekert protocol," *Phys. Rev. Lett.* **84**(20), 4733-4736 (2000).

⁷ C. H. Bennett and S. J. Wiesner, "Communication via one-particle and 2-particle operators on Einstein-Podolsky-Rosen states," *Phys. Rev. Lett.* **69**(20), 2881-2884 (1992).

⁸ C. H. Bennett, G. Brassard, C. Crepeau, A. Jozsa, A. Peres and

- W. K. Wootters, "Teleporting an unknown quantum state via dual classical and Einstein-Podolsky-Rosen channels," *Phys. Rev. Lett.* **70**(13), 1895–1899 (1993).
- ⁹ K. Mattle, H. Weinfurter, P.G.Kwiat and A. Zeilinger, "Dense coding in experimental quantum communication," *Phys. Rev. Lett.* **76** (25) 4656–4659 (1996).
- ¹⁰ D. Bouwmeester, J-W. Pan, K. Mattle, M. Eibl, H. Weinfurter and A. Zeilinger, "Experimental quantum teleportation," *Nature*, **390** (6660) 575–579 (1997).
- ¹¹ R. P. Feynman, "Simulating physics with computers," *Int. J. Theo. Phys.* **21** (6-7), 467-488 (1982).
- ¹² D. Deutsch and R. Jozsa, "Rapid solution of problems by quantum computation," *Proc. R. Soc. London A* **439**(1907), 553-558 (1992).
- ¹³ P. W. Shor, "Polynomial-time algorithms for prime factorization and discrete logarithms on a quantum computer," *SIAM J. Comput.* **26**(5), 1484-1509 (1997).
- ¹⁴ Michael A. Nielsen and Isaac L. Chuang, *Quantum computation and quantum information* (Cambridge U. Press, Cambridge, 2000).
- ¹⁵ P. G. Kwiat, K. Mattle, H. Weinfurter, A. Zeilinger, A. V. Sergienko and Y. H. Shih, "New high-intensity source of polarization-entangled photon pairs," *Phys. Rev. Lett.* **75**(24), 4337-4341 (1995).
- ¹⁶ P. G. Kwiat, E. Waks, A. G. White, I. Appelbaum, and P. H. Eberhard, "Ultrabright source of polarization-entangled photons," *Phys. Rev. A* **60**(2), R773-R776 (1999).
- ¹⁷ C. K. Hong and L. Mandel, "Theory of parametric frequency down conversion of light," *Phys. Rev. A* **31**(4), 2409-2418 (1985).
- ¹⁸ P. Hariharan and B. C. Sanders, "Quantum phenomena in optical interferometry," *Prog. Opt.* **36**, 49-128 (1996).
- ¹⁹ Robert W. Boyd, *Nonlinear optics* (Academic Press, Boston, MA, 1992).
- ²⁰ M. Ghioni, S. Cova, F. Zappa, and C. Samori, "Compact active quenching circuit for fast photon counting with avalanche photodiodes," *Rev. Sci. Instrum.* **67**(10), 3440-3448 (1996).
- ²¹ Perkin-Elmer Optoelectronics, SPCM-AQR Single-Photon Counting Module Data Sheet.
- ²² D. Dehlinger and M. W. Mitchell, "Entangled photons, nonlocality and Bell inequalities in the undergraduate laboratory," *Am. J. Phys.* **???** (???) ???-??? (???).